

Electronic topological transitions in Mo-Re random alloys

N. V. Skorodumova

Department of Theoretical Physics, Moscow Steel and Alloys Institute, Leninskii prospect 4, 117936, Moscow, Russia

S. I. Simak, I. A. Abrikosov, and B. Johansson

Condensed Matter Theory Group, Physics Department, Uppsala University, S-75121 Uppsala, Sweden

Yu. Kh. Vekilov

Department of Theoretical Physics, Moscow Steel and Alloys Institute, Leninskii prospect 4, 117936, Moscow, Russia

(Received 25 November 1997)

Electronic spectra and bulk properties of Mo-rich bcc Mo-Re random alloys have been studied in the framework of density-functional theory. We show that the Fermi surface topology changes with rhenium concentration, i.e., so-called electronic topological transitions take place. We have found two electronic topological transitions, the formation of an electronic void at about 2 at. % of Re and a formation of a neck at about 6 at. % of Re. The influence of these transitions on the thermodynamic (lattice parameter, bulk modulus, and Grüneisen constant) and kinetic (thermoelectric power) properties is analyzed. [S0163-1829(98)04120-4]

I. INTRODUCTION

The Fermi surface of a pure metal can be modified in different ways, for instance, by pressure or alloying. As a result the topology of the Fermi surface may change, i.e., voids or necks between different parts of the Fermi surface can appear or disappear. Lifshitz named such changes electronic topological transitions¹ (ETT's) and described them as $2\frac{1}{2}$ -order transitions using the Ehrenfest terminology.² He also pointed out that ETT's manifest themselves as certain anomalies in thermodynamic and kinetic properties of metals. The influence of ETT on physical properties of metallic systems has been investigated both experimentally and theoretically and the main results have been accumulated in a number of surveys.³⁻⁵

It is known that the Fermi surface changes its topology when the Fermi energy coincides with one of the critical energies corresponding to Van-Hove singularities in the electronic structure. This leads to the appearance of a singular contribution to the thermodynamic potential in such a way that its second derivative is continuous but the third one discontinuous at the transition point.¹ In pure metals at zero temperature this contribution occurs only at one side of the electronic topological transition but one needs to apply high pressure to study the effect. However, metals, especially transition metals, are normally quite hard and one can vary the electronic structure to a much smaller degree by applying pressure than, for example, by alloying. Therefore, probably the most interesting objects for investigation of ETT are metallic alloys. In the case of an alloy, however, all the anomalies are smeared out. This smearing may complicate the interpretation of the anomalies observed in physical properties. Thus, as a rule a theoretical investigation of the electronic spectra is needed. This has been done for a number of simple metal alloys⁶⁻⁸ as well as some alloys of transition metals.^{5,9-11}

In this paper we study the Fermi surface properties of random Mo-rich Mo-Re alloys as a function of Re concen-

tration. Electronic structure calculations of pure Mo show the existence of an unoccupied electronic branch slightly above the Fermi level along the NH line in the Brillouin zone (Fig. 1). Therefore, one can expect this branch to become populated when the d -band occupation is somewhat increased. This situation is easy to achieve by alloying Mo with an element from the higher neighboring group in the periodic table, for example, with Re [$\text{Mo}_{1-x}\text{Re}_x$ alloys form a homogeneous body-centered cubic (bcc) substitutional solid solution up to $x=0.2-0.42$ depending on temperature¹³]. As a

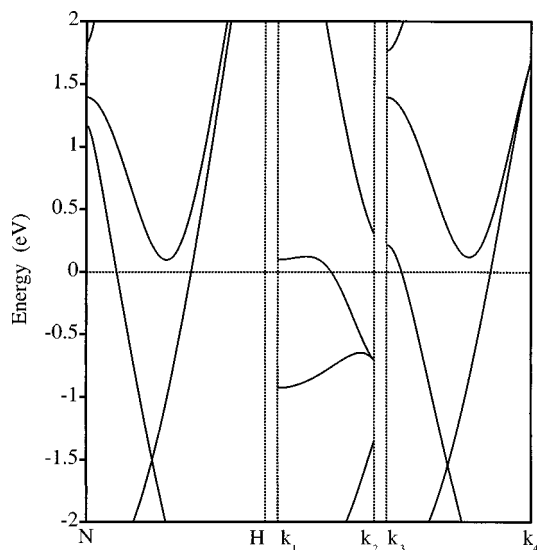


FIG. 1. Band structure of pure Mo at the calculated equilibrium lattice parameter obtained by the TB-LMTO method (Ref. 12) on the high-symmetry line NH as well as on the lines k_1k_2 [with coordinates (0.731,0.269,0) and (0.461,0,0) for k_1 and k_2 , respectively] and k_3k_4 [with coordinates (0.403,0.403,0) and (0.806,0,0) for k_3 and k_4 , respectively] (all coordinates are in units π/a , where a is the lattice parameter). The location of these lines in BZ is shown in Fig. 2. They are chosen in such a way that the electronic topological transition of the neck formation type takes place at their intersection (see Fig. 4). Energy is given relative to the Fermi level.

result the electronic topological transition should occur. As a matter of fact the experimental study of Mo-Re random alloys has revealed an anomaly of the thermopower at about 12 at. % of Re that could be an evidence of an ETT.¹⁴ On the other hand, the measurements of heat capacity¹⁵ have shown a quite monotonic dependence that makes one doubt the existence of an ETT in the system.

This contradiction has stimulated a number of theoretical studies of Mo-Re alloys. Starting from the information about the electronic spectra of pure Mo and using the rigid band model the authors of Ref. 14 connected the observed anomaly of the thermopower with some changes of the Fermi-surface topology. An attempt to study the Fermi surfaces of Mo-Re alloys in the framework of the coherent potential approximation–tight binding (CPA-TB) approach has been made in Ref. 16 but no ETT has been found. Bruno *et al.*⁵ have calculated the Fermi surfaces for two concentrations of Re (5 and 15 at. %) by means of the first-principles Korringa-Kohn-Rostocker (KKR)-CPA method. They showed that an electronic topological transition occurred within this concentration range but did not specify its type. At the same time the possibility of not one but a number of ETT's in the Mo-Re alloys has been suggested in Refs. 14 and 17. Thus, some further investigation seems to be necessary. We have studied the Fermi surfaces theoretically in the concentration range of 0–15 at. % of Re and shown how ETT's influence physical properties of the system.

To perform the actual electronic structure calculations we employed the self-consistent linear-muffin-tin-orbital (LMTO) method within the atomic-sphere (ASA) and the coherent-potential (CPA) approximations.^{18–26} Some details concerning the Fermi surface determination are given in Sec. II. The obtained electronic spectra, Fermi surfaces, and ground-state properties of the Mo-Re alloys at different concentrations are presented and discussed in Sec. III. A summary of the results is given in Sec. IV.

II. METHOD OF CALCULATION

A. Calculation of the Fermi surface of a random alloy within the LMTO-CPA method

The Fermi-surface determination for an ideal metal is a straightforward procedure. It is defined by those reciprocal space vectors k for which eigenstates $E_j(k)$ of the Hamiltonian are equal to the Fermi energy E_F . However, if there is no ideal periodicity, as in the case of a random alloy, the Hamiltonian approach becomes not very useful, and the Green's-function technique turns out to be more efficient.^{27,28} Unfortunately, in this case the direct information about the band structure is no longer available, and the determination of the Fermi surface has to be based on the calculation of the so-called Bloch spectral function $A^B(k, z)$ (BSF), which for a complex energy z and reciprocal space vectors k is given in terms of the Green's function as

$$A^B(k, z) = -\frac{1}{\pi} \text{Im} G(k, k, z), \quad (1)$$

where $G(k, k, z)$ is a Fourier transform of the corresponding real-space Green's function $G(r, r+R, z)$,²⁷ where R is the lattice site vector and r is the vector in the local coordinate

system centered at R . Having calculated the BSF one can locate its peaks positions. Thus an alloy “electronic band structure” and the Fermi surface may be determined, provided the properly averaged Green's function enters the right-hand side of Eq. (1).

However, in fact even one of the best approximations known to date, the coherent potential approximation, does not give the unique definition of the configuration averages for the non-site-diagonal properties like the Green's function $G(r, r+R, z)$. As a consequence a number of different approximations for calculating the BSF in the framework of the CPA have been put forward.^{27–30} In the present paper we have employed the approximation suggested in Refs. 29 and 30 which in the LMTO basis may be written (for a two-component $A_c B_{1-c}$ alloy) as

$$A(k, E) = -\frac{1}{\pi} \text{Im} \sum_L Q_L^\alpha(E) [\bar{P}^\alpha(E) - S^\alpha(k)]_{RL, RL}^{-1}, \quad (2)$$

where

$$Q_L^\alpha(E) = (P_L^{\alpha A} - P_L^{\alpha B})^{-1} \{ (P_L^{\alpha A} - \bar{P}_L^\alpha) \bar{P}_L^{\alpha B} - (P_L^{\alpha B} - \bar{P}_L^\alpha) \bar{P}_L^{\alpha A} \}. \quad (3)$$

In Eqs. (2) and (3) L is the combined angular-momentum quantum number (l, m) index, α denotes the LMTO representation, the structure constant matrix S contains all the information about the crystal structure, and the potential function for the alloy components $P^{\alpha j}$ ($j=A, B$) can be expressed by means of the band center C , bandwidth Δ , and γ LMTO potential parameters calculated at an arbitrary energy E_ν in the energy range of interest,²²

$$P_{Rl}^{\alpha j}(z) = \frac{C_{Rl}^j - z}{(C_{Rl}^j - z)(\gamma_{Rl}^j - \alpha_l) + \Delta_{Rl}^j}. \quad (4)$$

The potential function for the effective scatterers of the CPA effective medium \bar{P} is determined self-consistently from the CPA condition, which consists of the absence, on average, of electron scattering by the alloy components randomly distributed over the sites of this effective lattice,

$$\tilde{\mathbf{g}} = \sum_j c_j \mathbf{g}^j. \quad (5)$$

In Eq. (5) bold symbols denote $(RL, R'L')$ matrices, and $\tilde{\mathbf{g}}$ is the KKR-ASA Green's function for the ordered lattice of the effective scatterers,

$$\tilde{\mathbf{g}}^\alpha(z) = \int d^3k [\tilde{\mathbf{P}}^\alpha(z) - \mathbf{S}^\alpha(k)]^{-1}, \quad (6)$$

where c_j stands for the concentration of the alloy components, and \mathbf{g}^j is the Green's function of the j th alloy component considered as an impurity embedded into the ideal crystal formed by the effective scatterers. These Green's functions are given by the Dyson equation,

$$\mathbf{g}^j = [(\tilde{\mathbf{g}})^{-1} + \mathbf{P}^j - \tilde{\mathbf{P}}]^{-1}. \quad (7)$$

At this point we would like to remark that the use of Eq. (2) could sometimes lead to numerical problems associated

with the possibility of having poles of the potential function $P^{\alpha j}$, Eq. (4), in the energy region of interest that, in turn, leads to an appearance of unphysical singularities in the BSF. This problem has been discussed in the literature^{27,28} where an alternative approximation for the BSF has been put forward. On the other hand, it was also shown that for the energies where the potential function has no poles both approximations of the BSF give equivalent results. At the same time it is easy to check that in the framework of the TB-LMTO method the numerical pole problem can be simply eliminated by choosing an appropriate LMTO representation α , i.e., by changing the denominator in Eq. (4). Thus, one can shift a pole of the potential function off the energy region of interest. Our experience shows that normally there are no poles of P in the occupied part of the band if the most-localized representation is used. So it is quite safe to calculate the BSF following Eq. (2), which is simpler to use compared to the one given in Refs. 27 and 28.

B. Details of calculations

We performed the scalar-relativistic calculations with the basis set consisting of s , p , d , and f orbitals. Exchange and correlation were included within the local-density approximation using the Perdew-Zunger parametrization³¹ of the many-body calculations of Ceperley and Alder.³² The atomic sphere radii for both elements were chosen equal to the radius of the average atomic Wigner-Seitz sphere of the alloy. Charge-transfer effects, though small, were taken into account and the Madelung potential and energy were calculated in the framework of the screened impurity model with the prefactor $\beta=0.6$ for the Madelung energy.³³ To perform the Brillouin-zone (BZ) integration we took 2870 k points uniformly distributed in the irreducible wedge of bcc BZ. A great amount of k points was essential in this case for a proper treatment of the small regions of the BZ where ETT occurred. The energy integrals were calculated on a semicircular contour in the complex energy plane with 25 energy points on it distributed in such a way as to increase sampling near the Fermi energy. The convergence criterion for the total energy was 0.001 mRy. To obtain the ground state properties of the alloys we performed LDA self-consistent calculations for concentrations with 17 different lattice parameters, and subsequently used a Morse-like fitting for the total energy curves.³⁴ The BSF $A(k, E_F)$ was calculated at the equilibrium lattice parameters on a uniform grid of k points in the ΓNH and ΓHPN planes of the BZ. The density of states (DOS) has been calculated by means of the Green's-function technique, and the corresponding Green's function was evaluated for 1000 points distributed uniformly over the energy range of 0.8 Ry on a line in the complex energy plane parallel to the real axis, and was then analytically continued towards the real axis. Comparison with the conventional techniques carried out for pure bcc Mo shows that this is a reliable way to estimate both the density of states and its energy derivative.

III. RESULTS AND DISCUSSION

A. Fermi surfaces of Mo-Re alloys

In Fig. 2 we show the calculated sections of the Fermi

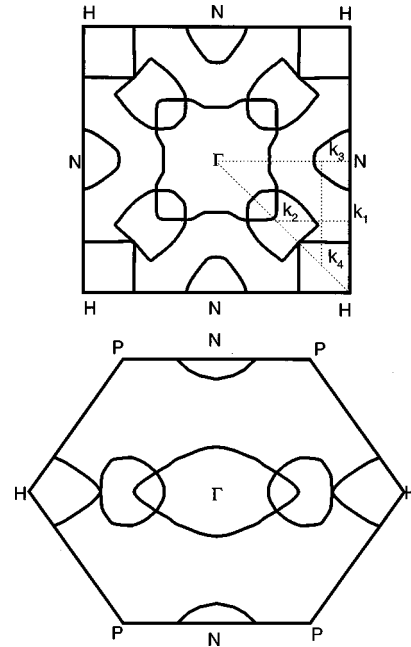


FIG. 2. The Fermi surface of pure Mo in the ΓNH and ΓHPN planes. Lines $k_1 k_2$ and $k_3 k_4$ are also shown (for details see caption to Fig. 1).

surface of pure Mo along the ΓNH and ΓHPN planes. Our results are in good agreement with earlier theoretical and experimental studies^{5,35} that demonstrate the reliability of our technique for the Fermi surface calculations.

When Re is added to Mo the Fermi surface topology visibly changes. This is a consequence of the fact that the unoccupied band situated near the NH line in pure Mo (Fig. 1) is crossed by the Fermi level. The addition of 2 at. % of Re is already sufficient to induce this crossing and, as a result, a new electronic void appears along the line NH (Fig. 3). This void grows quickly towards the electronic lens and at about 6 at. % of Re they conjoin forming a neck (Fig. 4). Therefore,

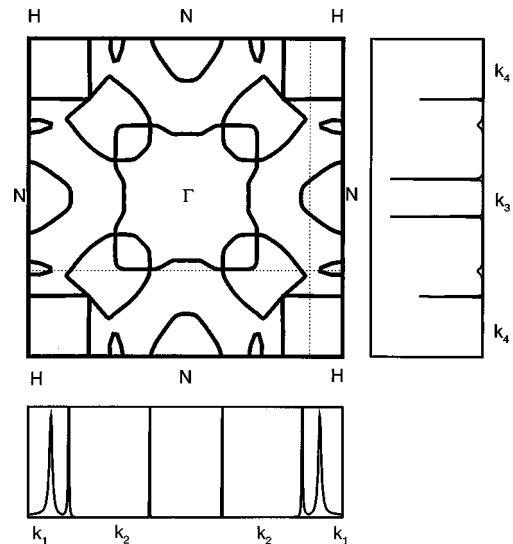


FIG. 3. The Fermi surface of $\text{Mo}_{98}\text{Re}_{02}$ alloy in the ΓNH plane. The bottom and the right panels show the Bloch spectral function in this alloy calculated along the dotted lines drawn in the main panel. Points k_1 , k_2 , k_3 , and k_4 are on these lines (for details see caption to Fig. 1).

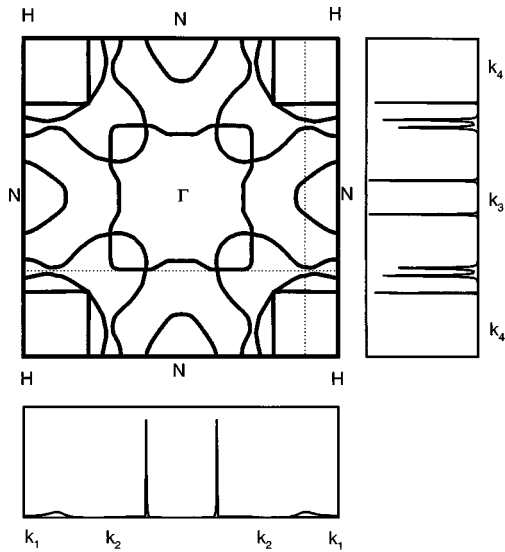


FIG. 4. The Fermi surface of $\text{Mo}_{94}\text{Re}_{06}$ alloy. Notations are the same as in Fig. 3.

there are two ETT's within a small concentration range: the appearance of a new void and a neck formation between the two electronic parts of the Fermi surface. Looking at the band structure of pure Mo along the lines k_1k_2 and k_3k_4 (indicated by dotted lines in Fig. 2), chosen in such a way that the neck formation takes place at their intersection, one can see (Fig. 1) the electronic band that becomes populated due to the increase of the electron concentration causing the formation of the neck. It is seen that along the line k_1k_2 this band has a rather flat fragment. This allows us to expect that the transition at 6 at. % of Re will give a bigger singular contribution to the DOS compared to the one at 2 at. % of Re where the new void forms.⁴

Let us remark here that this band is seen on the lines that are not high-symmetry lines and, therefore, it is not routinely presented in the discussions of band-structure results. This could be a reason why the transition of the neck formation type was not discussed in earlier studies of the Fermi surface of Mo-Re alloys.^{14,16,5}

To illustrate the neck formation process in detail we show the BSF calculated along two lines (shown by dotted lines in Figs. 3 and 4). These lines are identical to the lines k_1k_2 and k_3k_4 (Fig. 2). In Fig. 3 we present the situation for the $\text{Mo}_{98}\text{Re}_{02}$ alloy. In the bottom panel (k_1k_2 line) one can see two well-defined and separated BSF peaks. They correspond to the lens and the new void. The smearing of the BSF peaks due to disorder is very small but it gives rise to the slightly crossing tails. As a result a tiny peak has appeared on the line k_3k_4 shown in the right panel. The more Re we add, the closer the surfaces of the lens and the new void come to each other and, therefore, the more corresponding BSF peaks overlap. It takes some concentration range to get these two parts of the Fermi surface touched and then conjoined what means the formation of a neck between them. This situation is shown in Fig. 4 where one can see the BSF peaks corresponding to the two surfaces of the new neck (the right panel). They are already quite separated but still overlap a bit. This overlapping induces a small peak of the BSF on the line k_1k_2 (Fig. 4, the bottom panel).

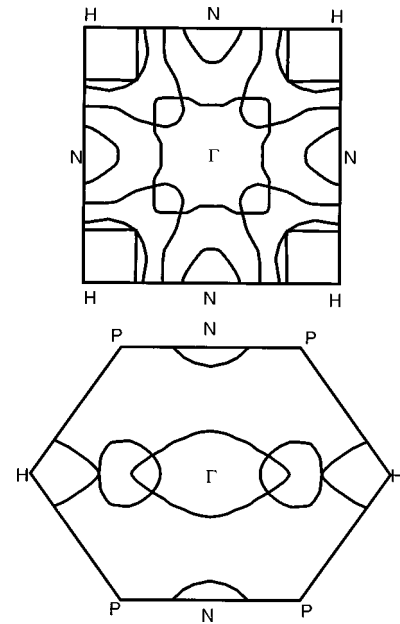


FIG. 5. The Fermi surface of $\text{Mo}_{88}\text{Re}_{12}$ alloy in the ΓNH and ΓHPN planes.

A further increase of the Re concentration leads to an expansion of the new neck but no other changes of the Fermi-surface topology are observed within the investigated concentration range (up to 15 at. % Re). To illustrate this we have presented the Fermi surface of the $\text{Mo}_{88}\text{Re}_{12}$ alloy in Fig. 5. We also remark that all the changes of the Fermi surface topology occur in the ΓNH plane. No changes are seen, for example, in ΓHPN plane (compare Figs. 2 and 5). Thus, from the above consideration one can conclude that in Mo-rich Mo-Re alloys there are two separate ETT of two different kinds.

B. Electronic topological transitions and the density of states

Let us discuss now the influence of the ETT on the physical properties of the system. The density of states for the $\text{Mo}_{94}\text{Re}_{06}$ alloy is shown in Fig. 6. It is seen that the Fermi level crosses a singularity of the DOS (shown by the arrow in Fig. 6). This happens at essentially the same concentration where the neck forms. Though the singularity is weak and smeared out by disorder, it clearly has a square-root shape, typical for ETT, and we conclude that it is induced by the transition of the neck formation type discussed above. But, as we expected, there is no comparable singularity corresponding to the formation of the new void. On the other hand, the peculiarities associated with this transition could be seen in those properties that are determined by the higher derivatives of the thermodynamic potential.

In Fig. 7 we show the logarithmic derivative of the density of states, $[1/N(E)][dN(E)/dE]$, at the Fermi level, plotted as a function of concentration (relative to the concentration corresponding to the transition of the neck formation type). One can see that there is a maximum at essentially the same alloy composition where the mentioned transition occurs. It is also known that in the framework of the simplest semiclassical theory the logarithmic derivative of the DOS is proportional to the thermoelectric power.³⁸ The qualitative

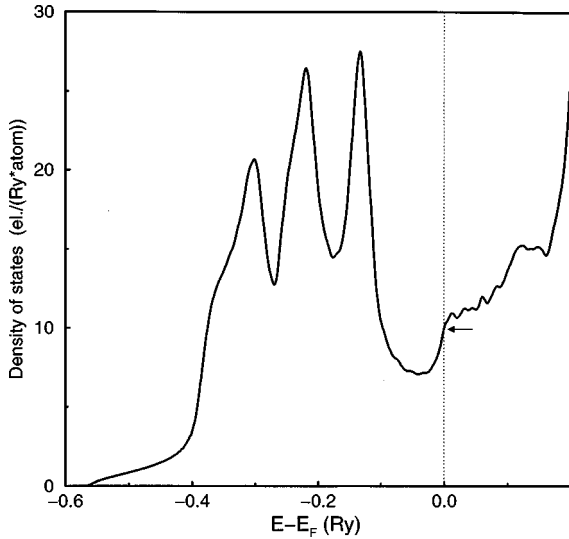


FIG. 6. Density of states of $\text{Mo}_{94}\text{Re}_{06}$ alloy. The Fermi energy is shown by the dotted line. The singularity of the DOS associated with the transition of the neck formation type is indicated with the arrow.

comparison of our results for the logarithmic derivative of the DOS and the experimentally measured thermopower taken from Ref. 14 are shown in Fig. 7. In the latter case we have chosen the concentration that corresponds to the maximum of the thermoelectric power, that is, 12 at. % of Re, as a reference concentration. Despite quantitative disagreement between this value and the concentration of the second ETT, clear similarities of the *concentration dependencies* of these two quantities allow us to conclude that there is a good qualitative agreement between them. As a matter of fact, the exact concentration at which the neck forms turns out to depend

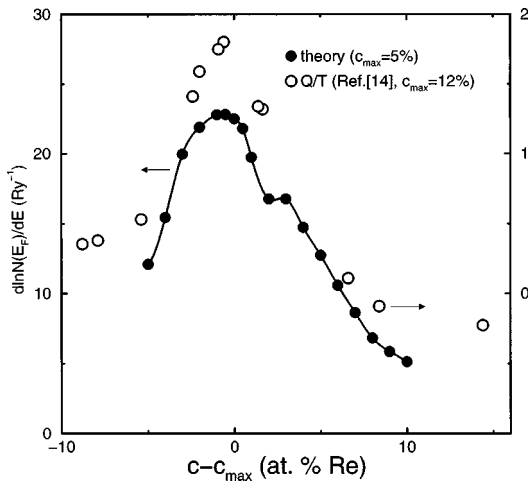


FIG. 7. Qualitative comparison of the concentration dependence of the logarithmic derivative of the calculated DOS (filled circles, full line) with the experimentally measured thermopower (open circles) (Ref. 14). The theoretical curve is plotted as a function of concentration relative to the concentration of the transition of the neck formation type ($c_{\max}=5\%$), its values are on the left axis (pointed to by an arrow). The experimental data are plotted relative to the concentration where the thermopower has its maximal value ($c_{\max}=12\%$); their values are on the right axis (pointed to by an arrow).

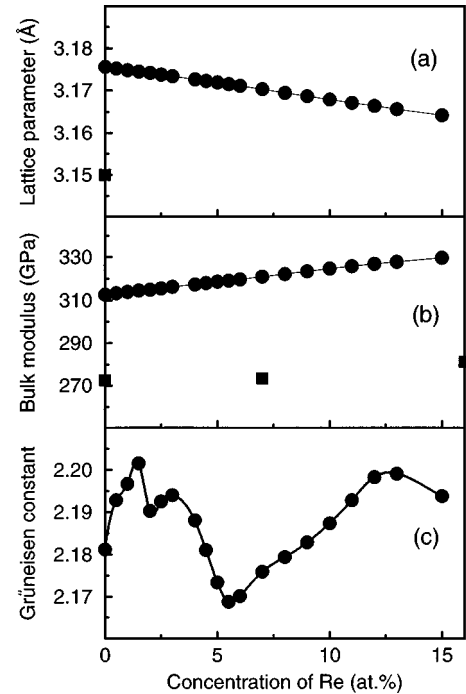


FIG. 8. Equilibrium lattice parameters (a), bulk moduli (b), and Grüneisen constants (c) of the Mo-rich Mo-Re alloys as a function of Re concentration. Calculated data are shown by filled circles. Experimental values for the lattice parameter (Ref. 36) and bulk modulus (Refs. 36 and 37) are shown by filled squares. The full line connecting the calculated values is given as a guide for the eye.

strongly on the computational setup. In particular, using the basis set of only s , p , and d orbitals we find that it occurs at about 16 at. % of Re. Unfortunately, it is known that there is a poor convergence of the LMTO calculations in the atomic-sphere approximation with respect to the l_{\max} , so one cannot be certain that our results with $l_{\max}=3$ are more accurate than those with $l_{\max}=2$. Nevertheless, they allow us to conclude that there are two ETT's that occur in a narrow concentration range upon alloying Mo with Re, and that the peculiarity of the thermoelectric power observed in Ref. 14 is associated with the formation of a neck rather than with the formation of a new void, as was believed earlier.

C. Electronic topological transitions and the ground-state properties

To study the influence of the found ETT on the ground-state properties of the Mo-Re alloys we have calculated their equilibrium lattice parameters, the bulk moduli, and the Grüneisen constants. In total we have considered 20 alloys with different concentrations up to 15 at. % of Re. Our calculated results together with the available experimental information are shown in Fig. 8. One can see that the calculated lattice parameter for pure Mo is slightly above the experimental one but the error is well within the typical accuracy of the LDA calculations. Moreover, the calculated bulk moduli well reproduce the experimental trend of this property.^{36,37} This situation is quite typical for the LMTO-CPA calculations using the LDA. Though the theory might not reproduce the right experimental values of the thermodynamic properties it normally gives a very good description of their trends.^{25,26}

Let us point out that, as a rule, the lattice parameter should not be affected by ETT but the bulk moduli and the Grüneisen constants could reflect some peculiarities because they are determined by the second and third derivatives of the thermodynamic potential, respectively. In fact, in pure metals at zero temperature ETT leads to square-root peculiarities of the bulk moduli. The Grüneisen constant must tend towards infinity at the points of ETT. In alloys disorder should smear out these peculiarities.¹ Therefore, the bulk modulus is not supposed to be a good test property for the study of ETT (notice that the second derivative of the thermodynamic potential is continuous at the point of the ETT even in the ideal case of a pure metal at zero temperature). Although the Grüneisen constant does not become infinite because of a disorder smearing it can show peculiarities that could be seen even in a disordered alloy.

As a matter of fact, this is what one may see in Fig. 8. The lattice parameters of the Mo-Re alloy decrease almost linearly with concentration, and the bulk moduli linearly increase. As expected, there is no visible square-root peculiarity in the concentration dependence of the bulk modulus but the concentration dependence of the Grüneisen constant [Fig. 8(c)] reveals obvious peculiarities at about 2 and 6 at. % Re that can be connected with the changes of the Fermi-surface topology at these concentrations.

IV. SUMMARY

The Fermi surface and the electronic properties of the bcc Mo-rich Mo-Re alloys have been studied by means of the

self-consistent LMTO-ASA-CPA method. The Fermi surfaces of the alloys are well defined and slightly smeared out by disorder. We have found two electronic topological transitions, the appearance of a new void at ~ 2 at. % of Re and the formation of a neck at ~ 6 at. % of Re.

The calculated concentration dependence of the logarithmic derivative of the alloy density of states at the Fermi level is found to be in good qualitative agreement with the experimental concentration dependence of the thermoelectric power. This allows us to conclude that an experimentally observed giant anomaly in the thermopower is connected to the transition of the neck formation type rather than the one associated with the appearance of a new void as was believed earlier. We have also studied the influence of the ETT on the thermodynamic properties of Mo-Re alloys, and found that the concentration dependence of the Grüneisen constant clearly demonstrates peculiarities associated with the ETT taking place in this system.

ACKNOWLEDGMENTS

We would like to thank Ya. M. Blanter for valuable discussions, and O. K. Andersen and O. Jepsen for letting us use the TB-LMTO code, which was applied for calculating the band structure of pure Mo. S.I.S., I.A.A., and B.J. are grateful to the Swedish Natural Science Research Council for financial support. The collaboration between Sweden and the former Soviet Union was supported by The Royal Swedish Academy of Sciences. RFFI Grant No. 98-0216419 is acknowledged.

-
- ¹I. M. Lifshitz, Zh. Eksp. Teor. Fiz. **33**, 1569 (1960) [Sov. Phys. JETP **11**, 1130 (1960)].
- ²P. Ehrenfest, Commun. Kamerlingh-Onnes Lab. Un. Leiden Suppl. **75B**, 813 (1933).
- ³A. A. Varlamov, V. S. Egorov, and A. V. Pantsulaya, Adv. Phys. **38**, 469 (1989).
- ⁴Ya. M. Blanter, M. I. Kaganov, and A. V. Pantsulaya, and A. A. Varlamov, Phys. Rep. **245**, 159 (1994).
- ⁵E. Bruno, B. Ginatempo, E. S. Giuliano, A. V. Ruban, and Yu. Kh. Vekilov, Phys. Rep. **249**, 355 (1994).
- ⁶V. G. Vaks, A. V. Trefilov, and S. V. Fomichev, Zh. Eksp. Teor. Fiz. **80**, 1613 (1981) [Sov. Phys. JETP **53**, 830 (1981)].
- ⁷G. Bruno, B. Ginatempo, E. S. Giuliano, and A. Stancanelli, Nuovo Cimento D **9**, 1495 (1987).
- ⁸S. S. Rajput, R. Prasad, R. M. Singru, W. Triftshauser, A. Eckert, G. Kogel, S. Kaprzyk, and A. Bansil, J. Phys.: Condens. Matter **5**, 6419 (1993).
- ⁹Yu. N. Gornostyrev, M. I. Katsnelson, G. V. Peschanskikh, and A. V. Trefilov, Phys. Status Solidi B **164**, 185 (1991).
- ¹⁰E. Bruno, B. Ginatempo, and E. S. Giuliano, Phys. Rev. B **52**, 14 557 (1995); **52**, 14 544 (1995).
- ¹¹N. V. Skorodumova, S. I. Simak, E. A. Smirnova, and Yu. Kh. Vekilov, Phys. Lett. A **208**, 157 (1995).
- ¹²The band structure of pure Mo was calculated using the code by G. Krier, M. van Schilfhaarde, A. T. Paxton, O. Jepsen, and O. K. Andersen, TIGHT-BINDING LMTO, version 4.6 (Max-Planck Institut, Stuttgart, 1994).
- ¹³R. Hultgren, P. D. Desai, D. T. Hawkins, M. Gleiser, and K. K. Kelley, *Selected Values of Thermodynamic Properties of Binary Alloys* (American Society for Metals, Metals Park, Ohio, 1973).
- ¹⁴A. N. Velikodnyi, N. V. Zavaritskii, T. A. Ignat'eva, and A. A. Yurgens, JETP Lett. **43**, 773 (1986).
- ¹⁵F. J. Morin and J. P. Maita, Phys. Rev. **129**, 1115 (1963).
- ¹⁶Yu. M. Yarmoshenko, G. V. Ganin, A. G. Narmonev, T. A. Ignat'eva, Yu. A. Cherevan', A. I. Zakharov, and E. Z. Kurmaev, Fiz. Met. Metalloved. **62**, 932 (1986).
- ¹⁷N. V. Skorodumova, S. I. Simak, Ya. M. Blanter, and Yu. Kh. Vekilov, JETP Lett. **66**, 549 (1994).
- ¹⁸O. K. Andersen, Phys. Rev. B **12**, 3060 (1975).
- ¹⁹O. Gunnarsson, O. Jepsen, and O. K. Andersen, Phys. Rev. B **27**, 7144 (1983).
- ²⁰H. L. Skriver, *The LMTO Method* (Springer-Verlag, Berlin, 1984).
- ²¹O. K. Andersen and O. Jepsen, Phys. Rev. Lett. **53**, 2571 (1984).
- ²²O. K. Andersen, O. Jepsen, and D. Glötzel, in *Highlights of Condensed-Matter Theory*, edited by F. Bassani, F. Fumi, and M. P. Tosi (North-Holland, Amsterdam, 1985).
- ²³O. K. Andersen, Z. Pawlowska, and O. Jepsen, Phys. Rev. B **34**, 5253 (1986).
- ²⁴I. A. Abrikosov, Yu. Kh. Vekilov, and A. V. Ruban, Phys. Lett. A **154**, 407 (1991).
- ²⁵I. A. Abrikosov, A. V. Ruban, D. Ya. Kats, and Yu. Kh. Vekilov, J. Phys.: Condens. Matter **5**, 1271 (1993).
- ²⁶I. A. Abrikosov and H. L. Skriver, Phys. Rev. B **47**, 16 532 (1993).

- ²⁷J. S. Faulkner and G. M. Stocks, *Phys. Rev. B* **21**, 3222 (1980).
- ²⁸J. S. Faulkner, *Prog. Mater. Sci.* **27**, 1 (1982).
- ²⁹G. M. Stocks, B. L. Györfy, E. S. Giuliano, and R. Ruggeri, *J. Phys. F* **7**, 1859 (1977).
- ³⁰W. M. Temmerman, B. L. Györfy, and G. M. Stocks, *J. Phys. F* **8**, 2461 (1978).
- ³¹J. Perdew and A. Zunger, *Phys. Rev. B* **23**, 5048 (1981).
- ³²D. M. Ceperley and B. J. Alder, *Phys. Rev. Lett.* **45**, 566 (1980).
- ³³P. A. Korzhavii, A. V. Ruban, I. A. Abrikosov, and H. L. Skriver, *Phys. Rev. B* **51**, 5773 (1995).
- ³⁴V. L. Moruzzi, J. F. Janak, and K. Schwarz, *Phys. Rev. B* **37**, 790 (1988).
- ³⁵R. Iverson and L. Hodges, *Phys. Rev. B* **8**, 1429 (1973).
- ³⁶V. L. Moruzzi, J. F. Janak, and A. R. Williams, *Calculated Electronic Properties of Metals* (Pergamon, Oxford, 1978).
- ³⁷D. L. Davidson and F. R. Brotzen, *J. Appl. Phys.* **39**, 5768 (1968).
- ³⁸N. W. Ashcroft and D. N. Mermin, *Solid State Physics* (Saunders College Publishing, Fort Worth, 1976), p. 257.